


Review

# Kinetics of Spreading over Porous Substrates

Phillip Johnson, Anna Trybala  and Victor Starov \*

Department of Chemical Engineering, Loughborough University, Loughborough LE11 3TU, UK;  
P.Johnson@lboro.ac.uk (P.J.); a.trybala@lboro.ac.uk (A.T.)

\* Correspondence: V.M.Starov@Lboro.ac.uk

Received: 18 January 2019; Accepted: 11 March 2019; Published: 15 March 2019



**Abstract:** The spreading of small liquid drops over thin and thick porous layers (dry or saturated with the same liquid) is discussed in the case of both complete wetting (silicone oils of different viscosities over nitrocellulose membranes and blood over a filter paper) and partial wetting (aqueous SDS (Sodium dodecyl sulfate) solutions of different concentrations and blood over partially wetted substrates). Filter paper and nitrocellulose membranes of different porosity and different average pore size were used as a model of thin porous layers, sponges, glass and metal filters were used as a model of thick porous substrates. Spreading of both Newtonian and non-Newtonian liquid are considered below. In the case of complete wetting, two spreading regimes were found (i) the fast spreading regime, when imbibition is not important and (ii) the second slow regime when imbibition dominates. As a result of these two competing processes, the radius of the drop goes through a maximum value over time. A system of two differential equations was derived in the case of complete wetting for both Newtonian and non-Newtonian liquids to describe the evolution with time of radii of both the drop base and the wetted region inside the porous layer. The deduced system of differential equations does not include any fitting parameter. Experiments were carried out by the spreading of silicone oil drops over various dry microfiltration membranes (permeable in both normal and tangential directions) and blood over dry filter paper. The time evolution of the radii of both the drop base and the wetted region inside the porous layer were monitored. All experimental data fell on two universal curves if appropriate scales are used with a plot of the dimensionless radii of the drop base and of the wetted region inside the porous layer on dimensionless time. The predicted theoretical relationships are two universal curves accounting quite satisfactorily for the experimental data. According to the theory prediction, (i) the dynamic contact angle dependence on the same dimensionless time as before should be a universal function and (ii) the dynamic contact angle should change rapidly over an initial short stage of spreading and should remain a constant value over the duration of the rest of the spreading process. The constancy of the contact angle on this stage has nothing to do with hysteresis of the contact angle: there is no hysteresis in the system under investigation in the case of complete wetting. These conclusions again are in good agreement with experimental observations in the case of complete wetting for both Newtonian and non-Newtonian liquids. Addition of surfactant to aqueous solutions, as expected, improve spreading over porous substrates and, in some cases, results in switching from partial to complete wetting. It was shown that for the spreading of surfactant solutions on thick porous substrates there is a minimum contact angle after which the droplet rapidly absorbs into the substrate. Unfortunately, a theory of spreading/imbibition over thick porous substrates is still to be developed. However, it was shown that the dimensionless time dependences of both contact angle and spreading radius of the droplet on thick porous material fall on to a universal curve in the case of complete wetting.

**Keywords:** porous; spreading; complete wetting; partial wetting

## 1. Introduction

In this review we briefly discuss recent advances in the kinetics of spreading of liquid droplets over porous substrates. Spreading of droplets over porous substrates is of great interest to various industries including coating, painting and printing. In the case of printing, understanding the kinetics of an ink droplet being deposited onto the paper and parameters affecting the spreading/imbibition of the liquid allows considerable improvement of printing methods.

The kinetics of spreading of droplets over smooth and none porous substrates is well documented [1–8]. However, this knowledge does not allow modelling the spreading behaviour over most materials due to their porous and rough nature of those materials. Addressing problem of spreading of droplets on permeable porous substrates is of interest for systems that involve spreading over textiles, spray-painting and printing on paper [9–17].

Porous substrates are characterised by their porosity, pore size, permeability and pore structure. Porous substrates with interconnected pores like paper, rock or sponge can be examined experimentally using confocal microscopy [18] and x-ray tomography [19]. There are a various models of porous substrates: In one-dimensional models the substrates are modelled as an array of capillaries of identical radii [20,21], Bethe lattice models, which accounts for interconnectivity [20], and Network models, which allow for the inclusion of interlinking pores along with the benefits discussed for the Bethe lattice model [22]. Improvements of the Network model have been made to include roughness into the system using the Koch curve and random walk [23] methods. However, the best-known models are based on equation/equations, which describe the liquid flow inside the porous substrates. The most frequently used are the Darcy model and Brinkman's model [13,14].

Below the problem of simultaneous spreading/imbibition of liquid droplets over porous substrates is briefly reviewed. The majority of real solids are rough to some degree, which can be modelled as covered by a thin porous layer, and/or covered with a porous layer. The presence of roughness and/or a porous layer changes the wettability of the substrate and the spreading behaviour [10,24–26]. Spreading and penetration of liquid droplets over a porous substrate is governed by gravitational, capillary and viscous forces [14,27,28]. If the drop size is small enough then the gravitational force is negligible and only the viscous and capillary forces contribute to the spreading/imbibition; porosity/permeability play an important role in this process [14].

In order to theoretically describe kinetics of simultaneous spreading and imbibition of droplets over a porous substrate, it is necessary to describe (i) the flow inside a droplet, (ii) the flow inside a porous substrate and (iii) these two flows should be coupled through boundary conditions at the droplet/porous substrate interface. This boundary conditions should include two conditions equality of velocities and equality of viscose stress at the droplet/porous substrate interface. The is no problem with the description of the flow inside a droplet, because this flow is described by Navie-Stokes equations in the case of Newtonian liquids [8] or its proper modifications in the case of non-Newtonian liquids [29,30], and application of these equations to the flow inside droplets is well-known. Flow inside the porous substrate is usually described based on Darcy equations [8]. However, Navie-Stokes equations (or their modifications in the case of non-Newtonian liquids) are second order differential equations and the Darcy equations are first order differential equations. That is, using Darcy equations it is impossible to satisfy two boundary conditions at the droplet/porous substrate interface.

The solution has been suggested as follows: To describe the flow inside the porous substrate using Brinkman's equations, which are the second order differential equations [31]. Hence, using Brinkman's equations (or their modification in the case of non-Newtonian liquid) it is possible to satisfy both boundary conditions at the droplet/porous substrate interface. It is the reason why Brinkman's Equations [32] are frequently used to describe the fluid flow in porous substrates. These equations are semi-empirical [31] with physically meaningful coefficients: an effective viscosity and a permeability coefficient. An attempt to use Brinkman's equations to describe the fluid flow inside a porous layer coupled with droplet flow over the layer has been undertaken in [33]. The same approach was used also in [14,34] for spreading of liquid drops over a thin porous substrate filled with the same liquid.

Brinkman equations modified for the case of non-Newtonian liquid were used in [29,30] to describe the blood flow inside the porous substrate at spreading of blood droplets over thin porous substrates (filter paper).

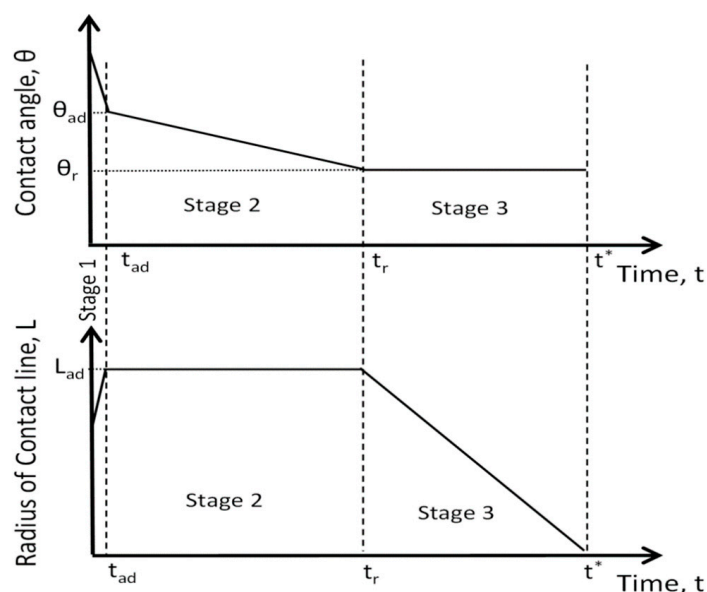
The effect of the thickness of the porous substrate is an important factor when considering the spreading of a droplet. In the case of printing the thin porous case is of relevance here but this has a different behaviour to the spreading over a thick porous substrate like porous rocks which is a more complex system. This additional complexity means that there is a lack of a complete theoretical understanding of the process that takes place within a thick porous substrate [35]. Thin porous substrates below means that the thickness of the porous substrate is much smaller as compared with a characteristic size of the droplet height.

When considering wettability, the effect of adding a surfactant is well known to improve the spreadability of a solution and how these change the kinetics of spreading over a porous substrate is discussed below. Inks in printing are generally enhanced with surfactants to control drop formation, spreading and imbibition into the substrate [8]. Below the spreading of pure liquids and aqueous surfactant solutions over various thin and thick porous substrates is discussed in the case of both Newtonian and non-Newtonian liquids. Two spreading behaviours are distinguished and revised: complete wetting and partial wetting cases.

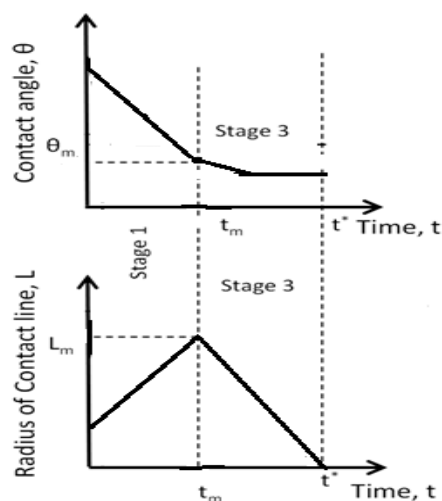
It is very straightforward to distinguish between the cases of complete and partial wetting in the case of spreading over non-porous substrates: In the case of complete wetting, the droplet spreads out completely but in the case of partial wetting the spreading stops after the static advancing contact angle is reached. It is not so straightforward to identify these two cases on the case of spreading over porous substrates. The way to distinguish complete wetting case from a partial wetting case during the spreading of drops over porous substrates was suggested in [14,35]. A schematics, which allow the distinguishing of the two different spreading regimes are shown in Figures 1 and 2. Figure 1 shows the partial wetting case: in this case three different spreading regimes are present. During the first stage, the contact angle decreases from the initial sufficiently high contact angle immediately after deposition until the static advancing contact angle is reached. After that the second stage starts: During this stage, the droplet base does not move, and the contact angle decreases almost linearly until the static receding contact angle is reached. Next, stage 3 starts: during this stage and until the end of the spreading/imbibition process, the contact angle remains constant and equals to the static receding contact angle. The above description of stages of spreading/imbibition in the case of partial wetting shows that the main feature of partial wetting is the presence of contact angle hysteresis.

Figure 2 shows a diagram of spreading stages in the complete wetting case where only two spreading regimes are present. The main feature of complete wetting is the absence of contact angle hysteresis. During the first stage the contact angle decreases, and the spreading area increases, until the max value of the spreading area is reached. During the second stage the contact angle remains almost constant, however, as shown in [14,35], the constancy of the contact angle during the second stage has nothing to do with contact angle hysteresis, which is absent in the case of complete wetting, but due to hydrodynamic reasons. The situation presented in Figures 1 and 2 was completely confirmed by experimental investigations (see below).

Note, the described above method to distinguish complete from partial wetting cases is equally applicable in the case of thin or thick porous substrates.



**Figure 1.** Schematics of three stages of spreading/imbibition of droplet over porous substrate in the case of partial wetting:  $L_{ad}$  is the maximum radius of droplet base,  $\theta_{ad}$  is the static advancing contact angle,  $t_{ad}$  is the time when  $\theta_{ad}$  is reached,  $\theta_r$  is the static receding contact angle,  $t_r$  is the time when  $\theta_r$  is reached and  $t^*$  is the time when spreading/imbibition is finished completely. [35].



**Figure 2.** Schematics of two stages of spreading/imbibition of droplet over porous substrates in the case of complete wetting:  $L_m$  is the maximum radius of droplet base,  $t_m$  is the time when  $L_m$  is reached,  $\theta_m$  is the contact angle at the moment  $t_m$ ,  $t^*$  is the time when complete imbibition is finished and  $\theta_f$  is the final contact angle at  $t^*$ . The contact angle  $\theta_f$  is completely determined by hydrodynamic reasons and has nothing to do with the static receding contact angle, because there is no contact angle hysteresis in the case of complete wetting [35].

## 2. Spreading over Thin Porous Substrates

### 2.1. Newtonian Liquids: Complete Wetting

Spreading of small droplets over a thin dry porous layer has been considered in [14]. The motion of a droplet over a porous layer is caused by the interaction of two processes: Spreading of the drop over the already saturated porous layer, which results in the expansion of the drop diameter and imbibition of the liquid from the drop into the porous substrate, which results in reduction of the drop diameter.

Imbibition expands the wetted region within the porous substrate. These two competing processes cause the drop diameter and hence radius of the droplet base to go through a maximum value. Under assumption on small porous substrate thickness allows simplifying the theoretical treatment considerably [14]. As a result, a system of two ordinary differential equations were derived to describe the evolution on time of both radius of the droplet base ( $L(t)$ ) and wetted area inside the thin porous substrate ( $l(t)$ ). The system includes two parameters one which accounts for the effective lubrication coefficient of the liquid over the wet porous substrate and the other is a combination of permeability and capillary pressure inside the porous layer [14,35,36]. Both parameters were determined in independent experiments [14], after that the system of equations does not include any fitting parameters.

In [14,35,36] the kinetics of spreading of a liquid droplet over the porous layer and imbibition into the layer was considered. A thin porous substrate is that has a thickness ( $\Delta$ ) much smaller than the drop characteristic height ( $h^*$ ) i.e.,  $\Delta \ll h^*$ . The drop is considered to have a low slope and the influence of gravity is assumed to be negligible. i.e., the only forces acting are capillary ones.

Kinetics of spreading of silicon oil of various viscosities over nitrocellulose membranes was experimentally investigated [14]. It was shown in [14] that the whole spreading process can be presented as shown in Figure 2, that is, corresponds to the complete wetting. It was shown in [8,14,37] that the first stage of the process is short enough (Figure 2), and capillary spreading prevails over droplet shrinkage caused by absorption into the porous layer. During the second stage, spreading almost stops, and the shrinkage of the droplet is determined by the suction of the liquid into the porous layer. It was also shown that during the second stage the contact angle remains constant, however, the latter has nothing to do with the contact angles hysteresis, because there is no contact angle hysteresis in the case of complete wetting. Based on the above assumptions a system of two interconnected ordinary differential equations was deduced in [14], for the radius of the droplet base,  $L(t)$ , and the radius of the wetted area inside the porous layer,  $l(t)$ . This system of differential equations was made dimensionless, which does not include any fitting parameters and hence predicts a universal behaviour on time of both the droplet base and the wetted area [14].

Experiments have been conducted which provide results consistent with the two stages of droplet spreading on a dry thin porous substrate [8]. A cellulose nitrate membrane was placed into a chamber and left to dry for 15 to 30mins, a light pulse was used to synchronise the time when the droplet started to spread to the cameras positioned. A droplet of silicone oil was placed onto the membrane and was measured until complete imbibition occurred. The silicone oils used were SO20, SO50, SO100 and SO500 [14].

For the kinetics of spreading for Newtonian liquids on thin porous substrates, the process is divided into two parts, fast spreading followed by a slow absorption. This is displayed theoretically in [14,35,36] and agrees with results from experimental investigations [14,27] (see Figures 3 and 4). Similar experimental work which agrees with the results shown in Figure 3 can be found in [37], where the contact angle of water droplets against time were tested on a OH-terminated self-assembled monolayer of thiol prepared on a gold-coated silicon wafer.

Figure 4 confirms the predicted theoretically universal behaviour of both the droplet base and the radius of the wetted area against time. These results are applicable to the spreading of inks on paper provided that the solution exhibits Newtonian characteristics and complete wetting behaviour. If the ink is non-Newtonian, the spreading behaviour changes and this is considered below.

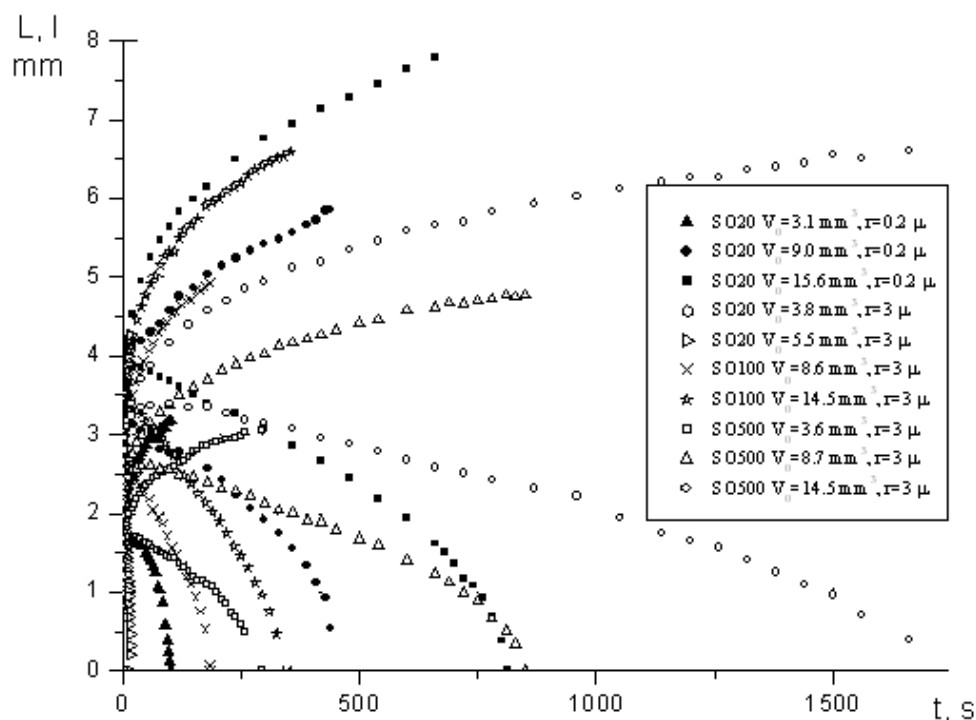


Figure 3. Measured dependencies of radii of the drop base ( $L$ , mm) and radii of the wetted region inside the porous layer ( $l$ , mm) on time ( $t$ , s). All relevant values are given in [14].

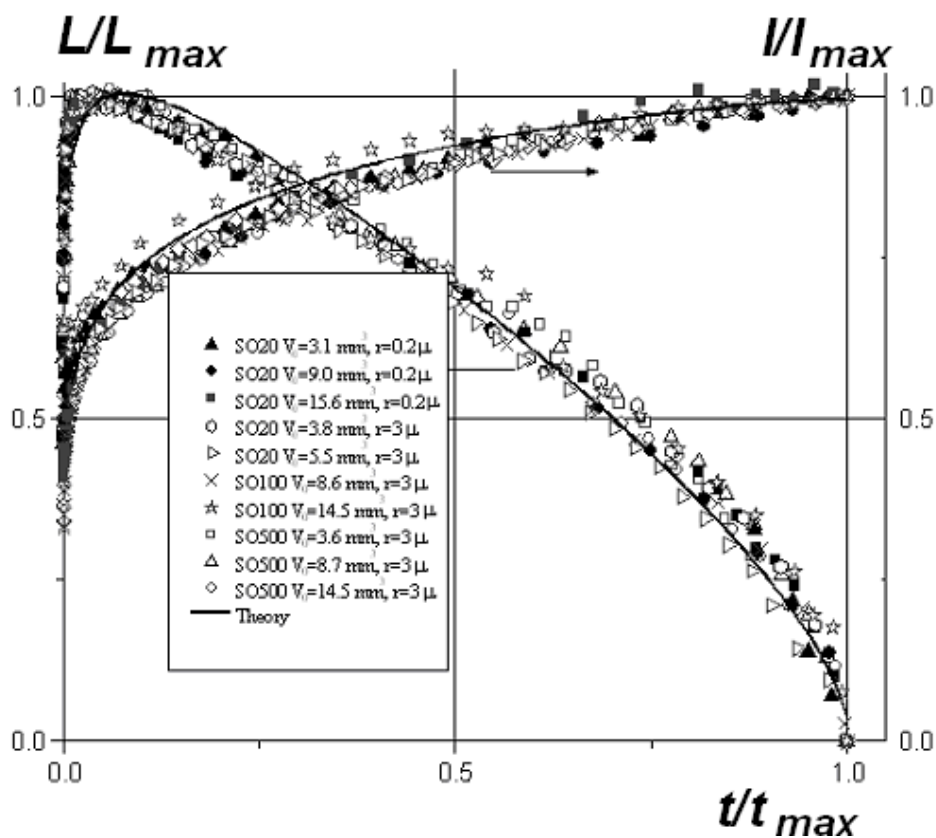


Figure 4. The same as in Figure 3 but using dimensionless co-ordinates: where  $L_{max}$  is the maximum value of the drop base, which is reached at the moment  $t_m$ . The scale  $l_{max}$  the time scale  $t_{max}$  are given in [13]. Solid lines according to the theoretical equations in [14].

## 2.2. Non-Newtonian Liquids: Complete and Partial Wetting Case

A non-Newtonian fluid is one that does not follow Newton's law of viscosity, which is constant viscosity independent of stress. In the case of a non-Newtonian fluid, viscosity can change when a force is being applied [27]. For spreading of non-Newtonian liquids there are also two possibilities as in the case of Newtonian liquids: complete and partial wetting.

It has been already described above how cases of complete and partial wetting can be distinguished when a liquid droplets spreads over porous substrates (Figures 1 and 2). This procedure is equally applied to both Newtonian and non-Newtonian liquids.

In the investigations carried out by Tzu Chieh Chao et al. [29,30,38] blood was used as the non-Newtonian liquid, to investigate the mechanisms of blood spreading during a dried blood spot (DBS) sampling procedure. Blood was found to show non-Newtonian power law shear thinning behaviour. DBS sampling is a method for collecting, transporting and storage which has been investigated in terms of clinical aspects in recent decades [39–44]. For example, developing and improving analytical methods. The procedure of DBS sampling consists of depositing a small known volume of blood on filter paper where it spreads and penetrates into the substrate. Meaning that the process is the spreading of blood, a non-Newtonian fluid, over a thin porous substrate. Presented in [29], blood droplets at a constant volume were deposited on filter paper and the radius of the wetted area measured with time. The whole spreading process was found to be described in two stages in the same way as Newtonian droplet spreading (Figures 3 and 4).

A system of two differential equations was derived for a non-Newtonian power law shear thinning liquid [29]. The system of equations describes the time evolution of both the radius of blood droplet base and the radius of the wetted region in the porous substrate. The universal behaviour of dimensionless dependencies of the radius of the droplet and the wetted region, also the contact angle, are almost independent of the rheological properties of blood. The results from the experiments in [29] fall on to this universal relationship showing a good agreement of simulated results with experimental data (Figures 5 and 6). During the whole spreading process the drop remained a spherical cap which agrees with the theory derived in [29]. It was found that both experimental and theoretical dependencies show a universal behaviour.

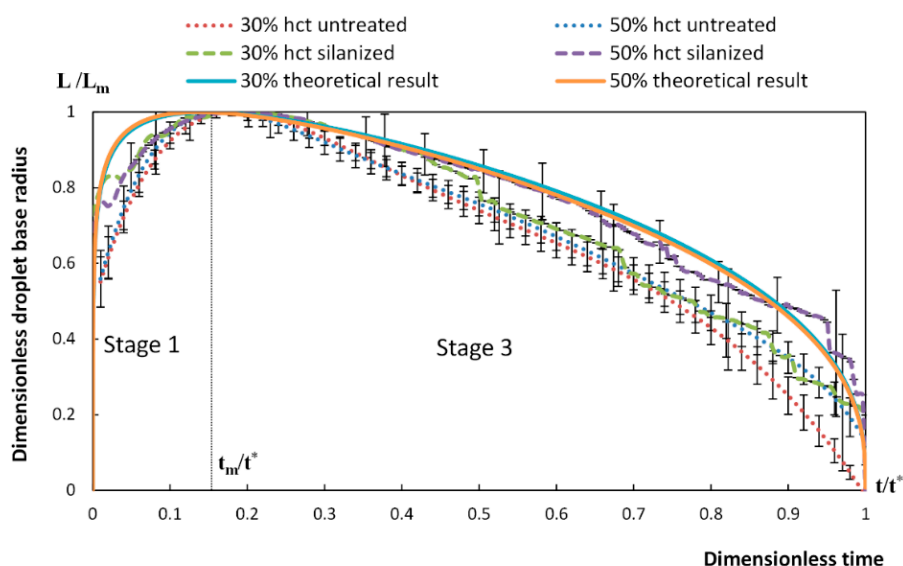


**Figure 5.** Dimensionless radius of the blood droplet base in the case of spreading over silanized and untreated Whatman 903 paper [29].

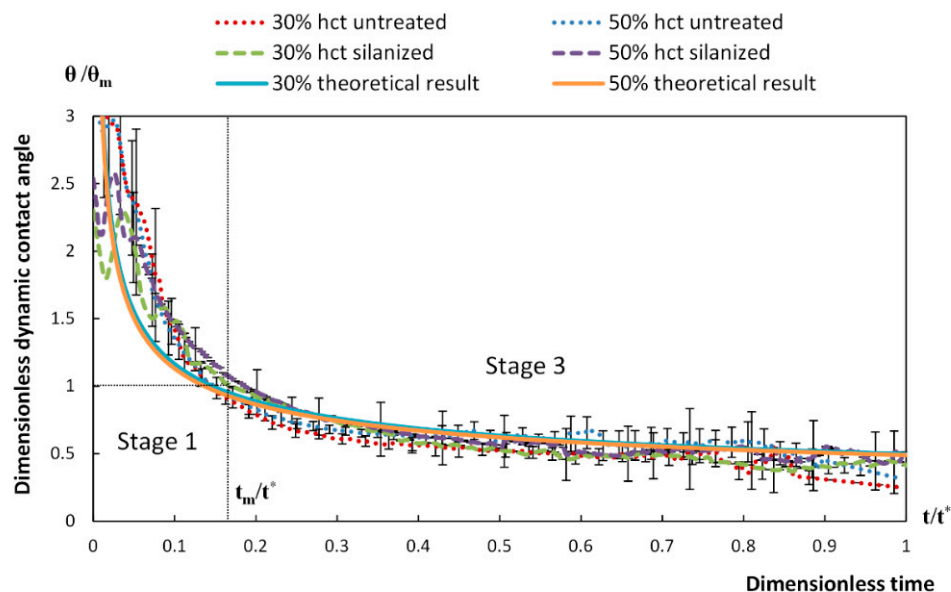


**Figure 6.** Dimensionless dynamic contact angle of blood droplet in the case of spreading over silanized and untreated Whatman 903 paper [35].

In [36], the spreading of non-Newtonian liquid (blood) droplets over a porous substrate, where only partial wetting occurs, was investigated. It was shown that the spreading can be divided into three stages, the same as was predicted earlier (Figure 1). The theory describes the spreading of droplets of Newtonian liquids on porous substrates which was modified in [36] for non-Newtonian liquids. Spreading of blood droplets on nitrocellulose membranes was investigated and it was shown that the blood droplets showed a partial wetting behaviour. The experimental results showed good agreement with the theoretical work discussed in [36], but also show that for membranes with pores smaller than  $0.2\mu\text{m}$ , smaller than the size of red blood cells, thus the red blood cells cannot penetrate and only the plasma can penetrate the substrate. The latter observation provides a way to separate red blood cells without damaging them. The partial wetting examples for dimensionless contact angle against time are shown in Figures 5 and 6, dimensionless droplet radius against time is shown by Figures 7 and 8 [36], which agrees with the schematic considerations shown in Figure 1.

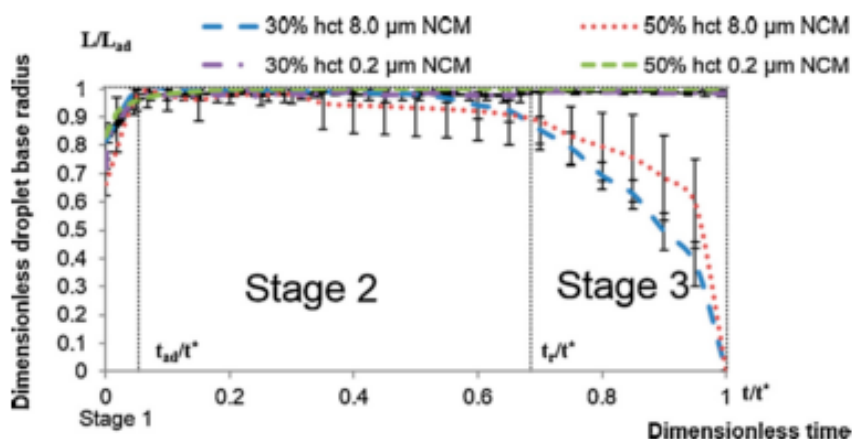


**Figure 7.** Dimensionless radius of the blood droplet base in the case of spreading over nitrocellulose membrane. In the case of  $0.2\mu\text{m}$  pores of nitrocellulose membrane only stage 1 and 2 are present [38].



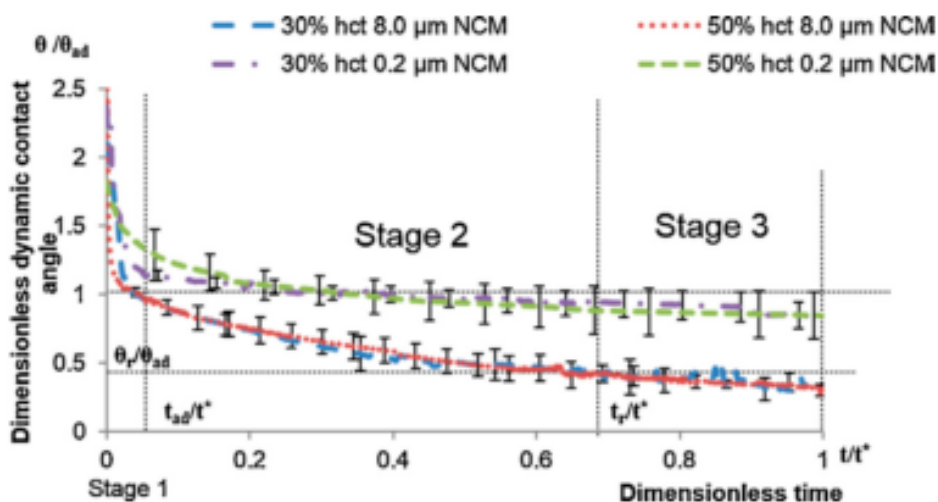


**Figure 8.** Dimensionless radius of contact angle in the case of spreading of blood droplets over nitrocellulose membrane. In the case of 0.2  $\mu\text{m}$  membrane pores there is no stage 3, it is a continuation of stage 2. The contact angle remained almost constant value after stage 1 [38].

### 3. Spreading over Thick Porous Substrates

Expanding on the work that was conducted on thin porous layers, work has been conducted using thick porous substrates completely wetted by silicone oils. In [15,35] these systems were experimentally investigated and the two stages as in Figure 2, were observed which correspond to the complete wetting case.

In [15] experiments were carried out observing the spreading of silicone oil droplets over multiple dry thick porous substrates the radius of the droplets and the wetted area of the substrates were monitored. All selected substrates were completely wetted by silicone oils (glass (thickness 1.9 mm to 2.5 mm) and metal (1.9 mm) filters).

It was shown that the process can be divided into stage in the same way as in the case of thin porous substrates. Experimental data proved that the spreading of silicone oil over dry thick porous substrates showed a universal behaviour if the appropriate dimensionless coordinates are introduced and for porous substrates made of different materials but with similar porosity and average pore sizes are used.

If the porous substrates of different porosity and average pore sizes were used, the dynamic radius of the drop base,  $L/L_{max}$ , and the radius of the wetted region on the surface,  $l/l_{max}$ , behave differentially during the spreading process. The wetted volume inside the porous substrate was unknown, however, to make possible a comparison if this volume was modelled as spherical cup of contact angle  $\psi$  (inside the porous substrates). However, the relative dynamic contact angle,  $\theta/\theta_{max}$  and the effective contact angle within the porous substrates,  $\psi/\psi_{max}$ , show also a universal behaviour [35].

### 4. Spreading of Surfactant Solutions over Porous Substrates

Surfactants lower both the liquid/air and the liquid/solid interfacial tensions, hence, increasing the spreadability

A partial wetting case was observed in all concentrations investigated using SDS aqueous solutions [45] on nitrocellulose porous membranes, however, for the spreading of the surfactant solutions the static receding contact angle was zero, which makes it similar to the complete wetting case. This was determined experimentally in [45] the process was separated into three stages [45]:

- Stage one: Drop base expands until a maximum value of drop base is reached and the contact angle rapidly decrease throughout this stage to the value of static advancing contact angle,  $\theta_{ad}$ .
- Stage two: Radius of the drop base remains constant and the contact angle decreases linearly with time until hydrodynamic receding contact angle is reached. Note, in the case the static receding

contact angle is equal to zero and the observed receding contact angle can be determined by hydrodynamic reasons only, like in the case of complete wetting.

- Stage three: The drop base shrinks and the contact angle remain constant until the complete disappearance of the drop.

The experimental work in [45] shows that the spreading time for droplets of SDS decreases as concentration increases. The difference between the advancing and receding contact angles decreases also with SDS concentration. The value of receding contact angle during stage three has nothing to do with hysteresis but determined by the hydrodynamic and spreading behaviour of the system becoming similar to complete wetting case. This is also observed in [17], which is discussed below in Section 5, where the addition of surfactant for droplets on sponges changes the spreading from a partial wetting case, for a distilled water droplet, to the complete wetting case for a surfactant solution droplet.

## 5. Spreading over Sponges

Sponges are an example for the spreading of liquid on thick porous substrates which is soft when compared to the other thick solid porous substrates discussed in Section 3. In [17], spreading of commercially available aqueous surfactant solutions on various sponges was investigated. Observation of the relationship between contact angle and concentration of surfactant solutions on different types of sponges was undertaken [17]. As discussed in Section 4, the influence of surfactants on wettability over solid porous substrates is known, it has also been observed that the addition of surfactants complicates the wetting process on solid porous substrates [44]. As mentioned previously there are two cases of spreading/imbibition process complete and partial wetting (see Figures 1 and 2).

Spreading of commercial surfactant on sponges [17] was investigated and both the contact angle and drop base diameter on different artificial sponges behaved on time. The sponges investigated were a dishwasher sponge (pore size:  $0.3017 \pm 0.0723$  and porosity: 0.689), audio sponge (pore size:  $0.09276 \pm 0.02814$  and porosity: 0.692) and a car sponge (pore size:  $0.2953 \pm 0.0704$  and porosity: 0.694). Spreading of distilled water on the sponges was found non-wetting case for both the dishwasher and car sponges which were both found to be hydrophobic (contact angle  $> 90^\circ$ ), whereas the audio sponge was found to be hydrophilic instantly absorbing the water.

For all of the sponges it was found that all the surfactant concentrations fell on universal curves for both dimensionless drop base diameter and dimensionless contact angle when plotted against dimensionless time [17]. Where dimensionless time is the value of time divided by the total time period, dimensionless drop base diameter is the diameter values divided by the maximum diameter of the droplet and dimensionless contact angle is the contact angle values divided by the maximum/initial contact angle. Figures 9 and 10 show the dimensionless curves for the audio and dishwasher sponges respectively. The same dependences for car sponge dimensionless curves are identical to that of the dishwasher sponge.

The above considered situation (Figures 9 and 10) is for the case of dry porous substrates. In both cases presented in Figures 9 and 10 spreading/imbibition behaviour correspond to the complete wetting case (Figure 2). In [17] spreading over pre-wetted sponges were also investigated. It was found that pre-wetting the sponges to any degree increases the rate of spreading. All sponges independent of the saturation all display a minimum critical contact angle, once reaching it, the droplet rapidly absorbed into the substrates. It was observed that initial contact angle and complete absorption contact angle depends on material behaviour more than degree of saturation.

Overall, it was observed in [17], that the contact angle and drop base diameter follow a universal behaviour, that the degree of pre-wetting affected the spreading rate and that the initial and absorption contact angle values were more dependent on the material and structural behaviour than the degree of pre-wetting.

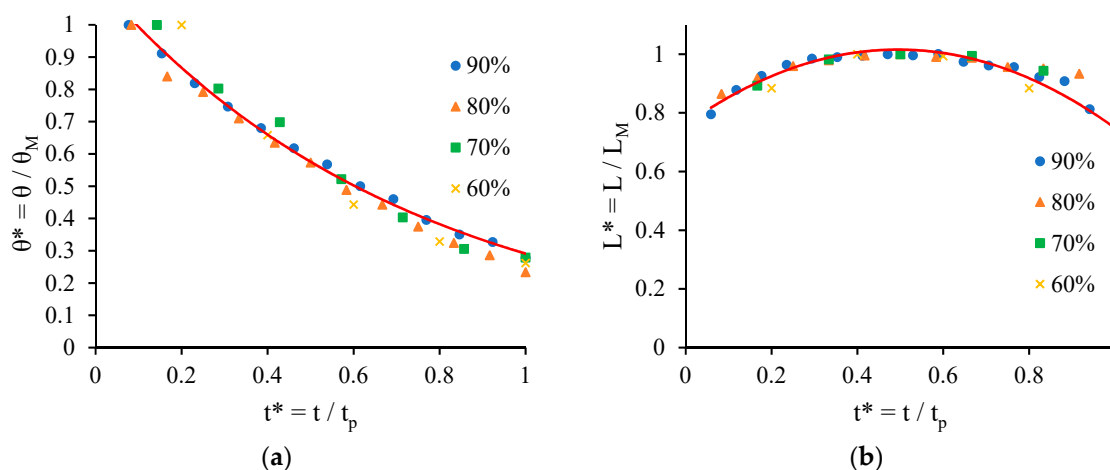


**Figure 9.** Contact angle (a) and droplet base diameter dimensionless (b) profiles for different percentage (%) concentrations of surfactants on dry audio sponge.

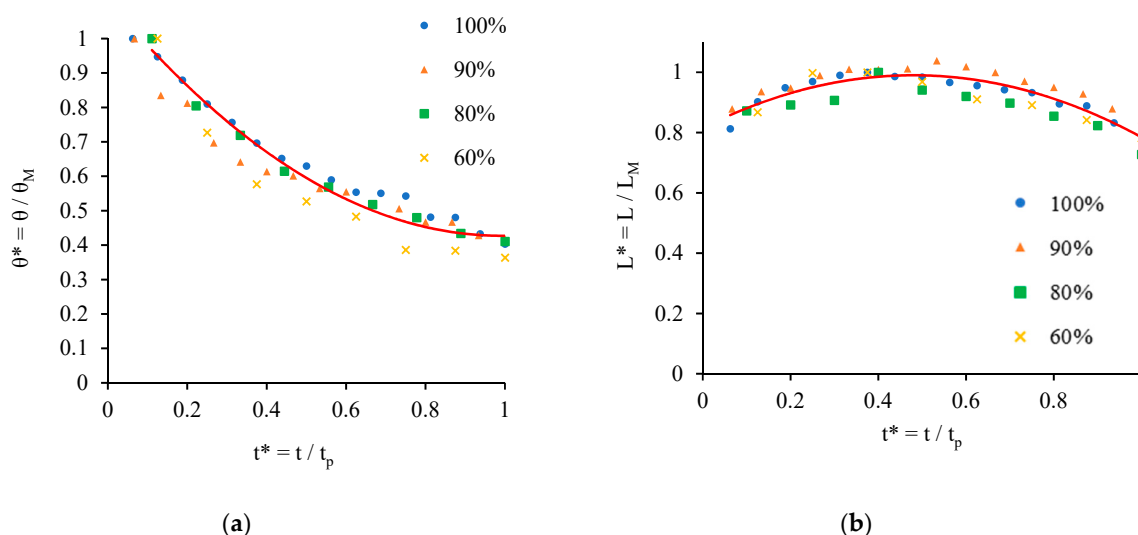


**Figure 10.** Contact angle (a) and droplet base diameter dimensionless (b) profiles for different percentage (%) concentrations of surfactants on dry dish sponge.

## 6. Conclusions

This review presents the current state of investigations of spreading of both Newtonian and non-Newtonian liquids over both thin and thick porous substrates. It is shown that a substantial progress has been made in investigation of spreading over thin porous substrates of both Newtonian and non-Newtonian liquid in the case of complete wetting. These processes have been investigated both theoretically and verified experimentally. Predicted universal theoretical dependences are in a good agreement with experimental observations in the case spreading/imbibition over completely wettable porous substrates in both the case of Newtonian and non-Newtonian droplets.

It was proven that in the case of partial wetting there are three stages of spreading, which are determined by the presence of contact angle hysteresis, there is an additional stage that is present where a slow imbibition into the substrate with the contact area remaining constant is present. It has also been shown that addition of surfactant to aqueous solutions improves the spreading and, in some cases, results in switching from partial to complete wetting.

The presence of a minimum contact angle in the case of spreading of surfactant solutions on thick porous substrates where it is found, after this contact angle is reached then the droplet rapidly absorbs into the substrate.

Further work is required for description of spreading of both Newtonian and non-Newtonian liquid over thick porous substrates; understanding of what determines the critical contact angle after which rapid absorption occurs. Spreading over porous substrates taking into account softness/deformability of the substrate is an area to be further developed.

**Author Contributions:** Conceptualization, A.T. and V.S.; writing—original draft preparation, P.J.; writing—review and editing, P.J., A.T. and V.S.; visualization, P.J. and V.S.; supervision, A.T. and V.S.; project administration, A.T.; funding acquisition, A.T. and V.S.

**Funding:** This research was supported by MULTIFLOW and CoWet EU grants, PASTA and MAP EVAPORATION European Space Agency grants, and a Proctor & Gamble grant.

**Conflicts of Interest:** The authors declare no conflict of interest. The funders had no role in the design of the study; in the collection, analyses, or interpretation of data; in the writing of the manuscript.

## References

1. Berg, J.C. *An Introduction to Interfaces and colloids The Bridge to Nanoscience*, 1st ed.; World Scientific Publishing Co.: Singapore, 2010.
2. Blokhuis, E.M.; Widom, B. Wetting. *Curr. Opin. Colloid Interface Sci.* **1996**, *1*, 424–429. [[CrossRef](#)]
3. Oron, A.; Davis, S.H.; Bankoff, S.G. Long-scale evolution of thin liquid films. *Rev. Mod. Phys.* **1997**, *69*, 931–980. [[CrossRef](#)]
4. De Gennes, P. Wetting: Statics and dynamics. *Rev. Mod. Phys.* **1985**, *57*, 827–863. [[CrossRef](#)]
5. Starov, V.M.; Kalinin, V.; Chen, J.-D. Spreading of liquid drops over dry surfaces. *Adv. Colloid Interface Sci.* **1994**, *50*, 187–221. [[CrossRef](#)]
6. Blake, T.D.; Haynes, J. Kinetics of liquid/liquid displacement. *J. Colloid Interface Sci.* **1969**, *30*, 421–423. [[CrossRef](#)]
7. Teletzke, G.; Davis, H.; Scriven, L. How Liquids Spread on Solids. *Chem. Eng. Commun.* **1987**, *55*, 41–82. [[CrossRef](#)]
8. Wijshoff, H. Drop dynamics in the inkjet printing process. *Curr. Opin. Colloid Interface Sci.* **2018**, *36*, 20–27. [[CrossRef](#)]
9. Washburn, F. The dynamics of capillary flow. *Phys. Rev.* **1921**, *17*, 273. [[CrossRef](#)]
10. Aradian, A.; Raphael, E.; de Gennes, P. Dewetting on porous media with aspiration. *Eur. Phys. J. E* **2000**, *2*, 367–376. [[CrossRef](#)]
11. Acton, J.; Huppert, H.; Worster, M.G. Two-dimensional viscous gravity currents flowing over a deep porous medium. *J. Fluid Mech.* **2001**, *440*, 359–380. [[CrossRef](#)]
12. Holman, R.K.; Cima, M.J.; Uhlund, S.A.; Sachs, E. Spreading and infiltration of inkjet-printed polymer solution droplets on a porous substrate. *J. Colloid Interface Sci.* **2002**, *249*, 432–440. [[CrossRef](#)] [[PubMed](#)]
13. Starov, V.M.; Kosvintsev, S.R.; Sobolev, V.D.; Velarde, M.G.; Zhdanov, S.A. Spreading of liquid drops over saturated porous layers. *J. Colloid Interface Sci.* **2002**, *246*, 372–379. [[CrossRef](#)] [[PubMed](#)]
14. Starov, V.M.; Kostvintsev, S.; Sobolev, V.D.; Zhdanov, S.A.; Velarde, M.G. Spreading of Liquid Drops over Dry Porous Layers: Complete Wetting Case. *J. Colloid Interface Sci.* **2002**, *252*, 397–408. [[CrossRef](#)] [[PubMed](#)]
15. Starov, V.M.; Zhdanov, S.A.; Velarde, M.G. Spreading of Liquid Drops over Thick Porous Layers: Complete Wetting Case. *Langmuir* **2002**, *18*, 9744–9750. [[CrossRef](#)]
16. Alleborn, N.; Raszillier, H. Spreading and Sorption of a Droplet on a Porous Substrate. *Chem. Eng. Sci.* **2004**, *59*, 2071–2088. [[CrossRef](#)]
17. Johnson, P.; Routledge, T.; Trybala, A.; Vaccaro, M.; Starov, V. Wetting and spreading of commercially available aqueous surfactants on porous materials. *Colloids Interfaces* **2018**, *3*, 14. [[CrossRef](#)]
18. Head, M.K.; Wong, H.S.; Buenfeld, N.R. Characterisation of ‘Hadley’ grains by confocal microscopy. *Cem. Concr. Res.* **2006**, *36*, 1483–1489. [[CrossRef](#)]
19. Peng, S.; Hu, Q.; Dultz, S.; Zhang, M. Using X-ray computed tomography in pore structure characterization for a Berea sandstone: Resolution effect. *J. Hydrol.* **2012**, *472–473*, 254–261. [[CrossRef](#)]
20. Sahimi, M. *Flow and Transport in Porous Media and Fractured Rock: From Classical Methods to Modern Approaches*; VCH Verlagsgesellschaft mbH: Weinheim, Germany, 1995.
21. Scheidegger, A. *The Physics of Flow Through Porous Media*, 3rd ed.; University of Toronto Press: Toronto, ON, Canada, 1974.

22. Lin, C.; Cohen, M.H. Quantitative methods for microgeometric modeling. *J. Appl. Phys.* **1982**, *53*, 4152–4165. [[CrossRef](#)]
23. Schwartz, L.M.; Banavar, J. Transport properties of disordered continuum systems. *Phys. Rev. B* **1989**, *39*, 16. [[CrossRef](#)]
24. Taniguchi, M.; Pieracci, J.; Belfort, G. Effect of Undulations on Surface Energy: A Quantitative Assessment. *Langmuir* **2001**, *17*, 4312–4315. [[CrossRef](#)]
25. Zdražil, A.; Stepanek, F.; Matar, O.K. Droplet spreading, imbibition and solidification on porous media. *J. Fluid Mech.* **2006**, *562*, 1–33. [[CrossRef](#)]
26. Bacri, L.; Brochard-Wyart, F. Droplet suction on porous media. *Eur. Phys. J. E* **2000**, *3*, 87–97. [[CrossRef](#)]
27. Kumar, S.M.; Deshpande, A.P. Dynamics of drop spreading on fibrous porous media. *Colloids Surf. A Physicochem. Eng. Asp.* **2006**, *277*, 157–163. [[CrossRef](#)]
28. Neogi, P.; Miller, C.A. Spreading kinetics of a drop on a rough solid surface. *J. Colloid Interface Sci.* **1983**, *92*, 338–349. [[CrossRef](#)]
29. Chao, T.C.; Arjmandi-Tash, O.; Das, D.B.; Starov, V.M. Spreading of blood drops over dry porous substrate: Complete wetting case. *J. Colloid Interface Sci.* **2015**, *446*, 218–225. [[CrossRef](#)] [[PubMed](#)]
30. Chao, T.C.; Trybala, A.; Starov, V.; Das, D.B. Influence of haematocrit level on the kinetics of blood spreading on thin porous medium during dried blood spot sampling. *Colloids Surf. A Physicochem. Eng. Asp.* **2014**, *451*, 38–47. [[CrossRef](#)]
31. Whitaker, S. *The Method of Volume Averaging*; Kluwer Academic Publishers: Dordrecht, The Netherlands; Boston, MA, USA; London, UK, 1999.
32. Brinkman, H. The Viscosity of Concentrated Suspensions and Solutions. *J. Chem. Phys.* **1952**, *20*, 4. [[CrossRef](#)]
33. Zhdanov, V.G.; Starov, V.M. Calculation of the effective properties of porous and composite materials. *Colloid J. Russ. Acad. Sci. Kolloidn. Zhurnal* **2002**, *64*, 783–792.
34. Kornev, K.G.; Neimark, A.V. Spontaneous penetration of liquids into capillaries and porous membranes revisited. *J. Colloid Interface Sci.* **2001**, *235*, 101–113. [[CrossRef](#)] [[PubMed](#)]
35. Starov, V.; Velarde, M.; Radke, C. *Dynamics of Wetting and Spreading*, 1st ed.; Taylor & Francis: Oxford, UK, 2007.
36. Koursari, N.; Arjmandi-Tash, O.; Johnson, P.; Trybala, A.; Starov, V.M. Foam Drainage Placed on a Thin Porous Layer. *Soft Matter* **2015**, *11*, 3643–3652.
37. Drelich, J.; Chibowska, D. Spreading kinetics of water drops on self-assembled monolayers of thiols: Significance of inertial effects. *Langmuir* **2005**, *21*, 7733–7738. [[CrossRef](#)] [[PubMed](#)]
38. Chao, T.C.; Arjmandi-Tash, O.; Das, D.B.; Starov, V.M. Simultaneous spreading and imbibition of blood droplets over porous substrates in the case of partial wetting. *Colloids Surf. A Physicochem. Eng. Asp.* **2016**, *505*, 9–17. [[CrossRef](#)]
39. Meesters, R.J.; Hooff, G. State-of-the-art dried blood spot analysis: An overview of recent advances and future trends. *Bioanalysis* **2003**, *5*, 17. [[CrossRef](#)] [[PubMed](#)]
40. Edelbroek, P.M.; van der Heijden, J.; Stolk, L.M.L. Dried Blood Spot Methods in Therapeutic Drug Monitoring: Methods, Assays, and Pitfalls. *Ther. Drug Monit.* **2009**, *31*, 327–336. [[CrossRef](#)] [[PubMed](#)]
41. Demirev, P.A. Dried blood spots: Analysis and applications. *Anal. Chem.* **2013**, *85*, 779–789. [[CrossRef](#)] [[PubMed](#)]
42. Snijdewind, I.J.M.; van Kampen, J.J.A.; Fraaij, P.L.A.; van der Ende, M.E.; Osterhaus, A.D.M.E.; Gruters, R.A. Current and future applications of dried blood spots in viral disease management. *Antivir. Res.* **2012**, *93*, 309–321. [[CrossRef](#)] [[PubMed](#)]
43. Tanna, S.; Lawson, G. Analytical methods used in conjunction with dried blood spots. *Anal. Methods* **2011**, *3*, 1709–1718. [[CrossRef](#)]
44. Lehmann, S.; Delaby, C.; Vialaret, J.; Ducos, J.; Hirtz, C. Current and future use of ‘dried blood spot’ analyses in clinical chemistry. *Clin. Chem. Lab. Med.* **2013**, *51*, 1897–1909. [[CrossRef](#)] [[PubMed](#)]
45. Zhdanov, S.A.; Starov, V.M.; Sobolev, V.D.; Velarde, M.G. Spreading of aqueous SDS solutions over nitrocellulose membranes. *J. Colloid Interface Sci.* **2003**, *264*, 481–489. [[CrossRef](#)]

